

UCSF

UC San Francisco Electronic Theses and Dissertations

Title

The mechanics governing epithelial morphology during *Drosophila melanogaster* oogenesis

Permalink

<https://escholarship.org/uc/item/8m3358p8>

Author

Shreter, Daniel

Publication Date

2008

Peer reviewed|Thesis/dissertation

The Mechanics Governing Epithelial Morphology during
Drosophila melanogaster Oogenesis

by

Daniel Shreter

Thesis

Submitted in partial satisfaction of the requirements for the degree of

MASTER OF SCIENCE

in

Bioengineering

in the

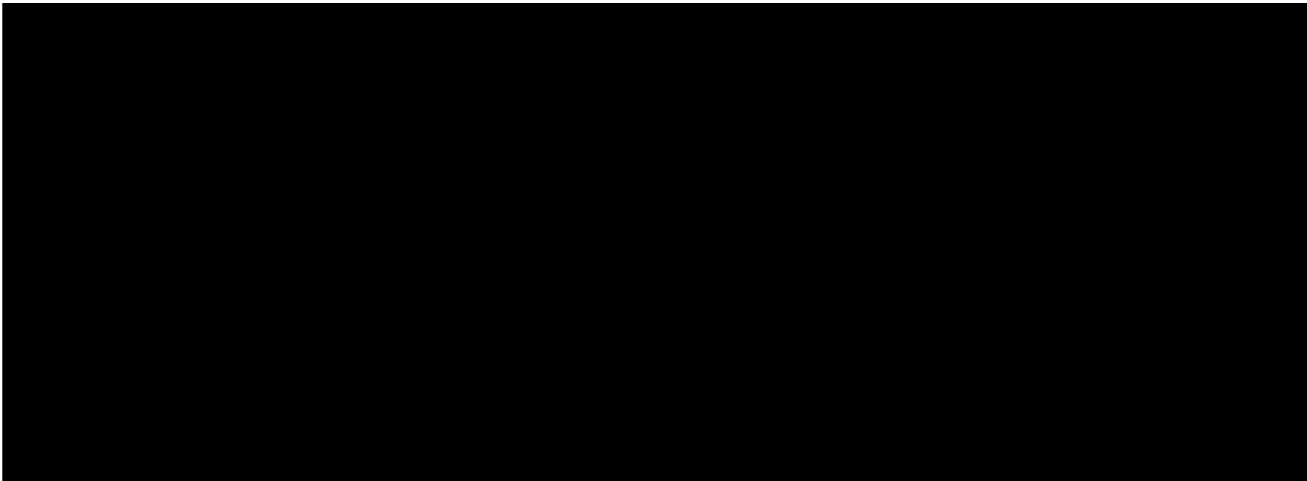
GRADUATE DIVISION

of the

UNIVERSITY OF CALIFORNIA, SAN FRANCISCO

AND

UNIVERSITY OF CALIFORNIA, BERKELEY



Date

University Librarian

Degree Conferred:

Acknowledgements

I would like to thank my research advisor, Mohammad Kaazempur-Mofrad, for his guidance and dedication to this research. He was extremely supportive, and helped me add another definition for biomechanics. As well, David Bilder welcomed me into his lab where his experience with *Drosophila* was invaluable to this research.

Anne Classen may be the most helpful and eager person ever, and it was a pleasure to work with her. Conversations with Sally Horne-Badovinac and the rest of the Bilder lab were extremely valuable as well.

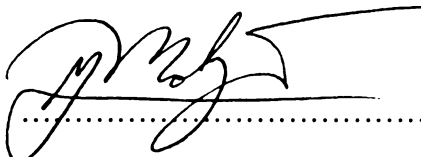
The members of the Mofrad lab made the lab a fun place to hang around, and they also contributed discussion and ideas to this research. Specifically, I would like to thank Kevin Kolahi for his help with experimental work, and Vimalier Reyes-Ortiz for his illustration.

The Mechanics Governing Epithelial Morphology during *Drosophila melanogaster* Oogenesis

By Daniel Moshe Shreter

Abstract

During *Drosophila melanogaster* oogenesis, the follicle cell epithelium (FCE) undergoes a variety of mechanically interesting processes. Included in oogenesis is the so-called posterior migration of the FCE, whereby the initially homogeneous epithelium segregates into a population of columnar cells over the oocyte and a population of squamous cells over the nurse cells. This ‘posterior migration’ has previously been attributed to apical constriction of the columnar cells, enabling them to tightly localize over the oocyte surface. Contrary to the previously hypothesized mechanism, our data indicate that the behavior of the two populations of follicle cells can be attributed to differential stretch, and we have demonstrated this through a combination of morphometric characterization of the FCE and finite element mechanical modeling. Within our computational model for the FCE, time varying viscoelastic properties and growth rather than apical constriction or cell motility account for the bulk of the shape changes observed during ‘posterior migration’.



.....
Mohammad Kaazempur-Mofrad, Thesis Committee Chairman

Table of Contents

Introduction.....	1
1. <i>Epithelia and cell migration as motivations for this research</i>	1
2. <i>Oogenesis, the follicle cell epithelium, and posterior migration</i>	2
3. <i>Overall project goals</i>	7
4. <i>The goal of this thesis</i>	7
Past characterizations of stage 9 follicle cell displacement	9
1. <i>Posterior migration</i>	9
2. <i>Follicle cell displacement depends upon oocyte positioning</i>	9
3. <i>Apical constriction as a hypothesis for posterior displacement</i>	10
Morphometric characterization of the follicle cell epithelium	12
1. <i>Introduction</i>	12
2. <i>Fly Stocks</i>	12
3. <i>Drosophila strains</i>	13
4. <i>Dissection</i>	14
5. <i>Fixation and staining</i>	15
6. <i>Confocal Imaging</i>	17
7. <i>Morphometric analysis</i>	17
8. <i>Results</i>	18
9. <i>Conclusions</i>	21
Previous work in developmental mechanics modeling.....	24
Mechanical description of the FCE and germline cells during oogenesis	27
1. <i>FCE cytoskeletal and adhesive structures</i>	27

2.	<i>Active force generation and myosin</i>	29
3.	<i>Apical and basolateral division of cell domains</i>	30
4.	<i>Material properties</i>	31
5.	<i>Germline characterization</i>	32
6.	<i>Anterior-posterior elongation</i>	33
7.	<i>Initial and final state of the system</i>	34
	Finite element model implementation	36
1.	<i>Preprocessor and solver</i>	36
2.	<i>Material model</i>	36
3.	<i>Forces exerted by the germ-line</i>	39
4.	<i>Meshing and solution</i>	39
5.	<i>Results and discussion</i>	40
6.	<i>Conclusions and future work</i>	43
	References	46

Introduction

1. Epithelia and cell migration as motivations for this research

Epithelium is one of four basic tissue types found within humans and other organisms. Epithelia can be found lining the inner and outer surface of all organs, performing a variety of specialized functions including secretion, compartmentalization, absorption, protection, and mechanosensation (Chan, 2001).

These functions are fundamentally related to epithelial architecture, which is defined by these cells' ability to form layers. Epithelia are polarized with apical and basolateral domains that are separated by an adhesive band called the *zonula adherens*. This structure serves as an important boundary between the structurally and functionally different regions of the cell.

Although epithelium can be found in a variety of structures and performing varied functions, its morphogenetic behavior during development is especially interesting. During embryonic development, the epithelia are highly dynamic and are of primary importance to the morphogenesis of the organism and the early reshaping of two-dimensional tissues into three-dimensional organs. The ability of epithelium to generate dramatic shape changes is driven in part by cytoskeletal activity and cell-cell and cell-substrate adhesion. In adult epithelium, cytoskeleton and cell adhesion properties are also the primary determinants of morphology, an important characteristic of these cells, which can be found in a variety of shapes including squamous, cuboidal, and columnar.

Of significant biomedical relevance is epithelium's ability to migrate. Understanding migratory behavior has implications as varied as wound healing, tumor metastasis, and tissue engineering (Lauffenburger and Horwitz, 1996). Migration is especially interesting to study because of its pronounced multidisciplinary nature. The molecular basis, biological behavior, and underlying mechanics are all subjects of study, and our research includes aspects of all three.

2. Oogenesis, the follicle cell epithelium, and posterior migration

A particularly interesting epithelial structure is the follicle cell epithelium (FCE) found in *Drosophila melanogaster* oogenesis. Oogenesis is the process of developing a mature oocyte within the ovary (Figure 1). The mature oocyte produced by this process is a germ cell encased by an egg shell that protects it from the external environment.

The production of the egg chamber begins at the germarium. Each germarium contains two populations of stem cells: typically two germline stem cells and two somatic stem cells. Each division of a germline stem cell yields a cystoblast. The cystoblast is pushed posteriorly through the germarium as more cystoblasts are created. As the cystoblasts are formed, they continue to divide until after 4 divisions they consist of a 16 cell cyst of germ cells interconnected by ring canals. Concurrent with the production of the germ cells is the division of the somatic stem cells. These produce follicle cell (FC) precursors that encapsulate the 16 cell cyst (Margolis and Spradling, 1995). These follicle cell precursors line the walls of the germarium as they move posterior from the somatic stem cells. After encapsulation, the egg chamber emerges from the germarium. The

surrounding FCs are in a single layer of cuboidal cells that are nearly uniform over the surface.

Within the egg chamber, the oocyte is not easily distinguishable from the other 15 germline cells; however, the posterior localization of the oocyte is an essential event that occurs early during oogenesis. The oocyte undergoes a cell-sorting event driven by upregulated expression of E-cadherin in both the oocyte and posterior FCs (Godt and Tepass, 1998). For approximately the first 80 hrs of oogenesis, stages 1-8, the FCs remain morphologically similar, although the cells are being patterned along the anterior-posterior (A-P) axis, and undergoing proliferation, growth, and endoreplication. Through stage 6, the FCs remain similar in size, but proliferation occurs along with germ cell growth until there are approximately 900 follicle cells (Drummond-Barbos and Spradling, 2001). During stage 7-8, the FCs no longer proliferate, and instead undergo endoreplication and growth in order to keep up with the enlarging germ cells.

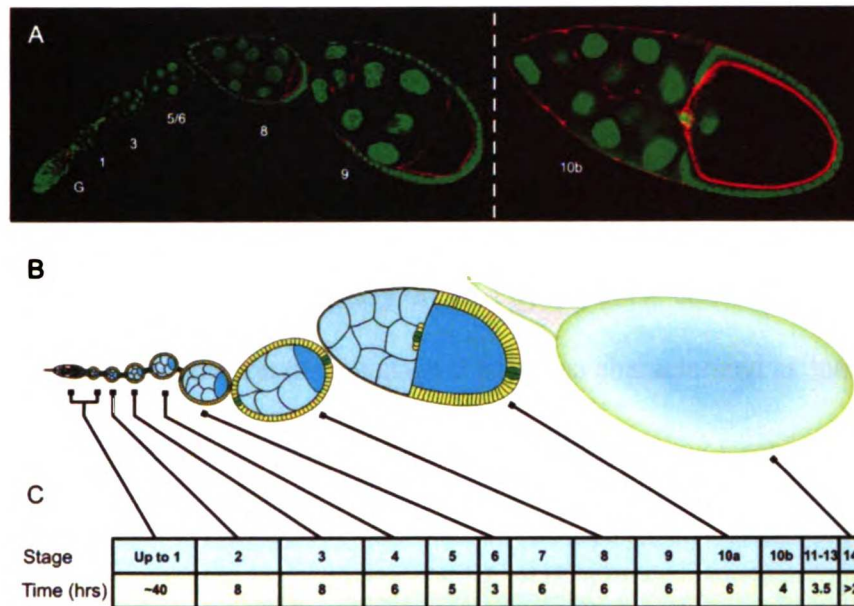


Figure 1. Overview of Drosophila oogenesis. Oogenesis begins at the germarium, where stem cells give rise to the germ cells and somatic cells of the developing follicle. The egg chambers are organized in sequential stages of development as they pass down the ovariole. A: The number below each egg chamber indicates the stage of oogenesis. B: In stages 1-8, the FCE retains a cuboidal shape. In stages 5-10, a variety of processes can be seen including anterior-posterior elongation and the posterior movement of the follicle cells. C: Timeline of the stages of oogenesis (Figure from Horne-Badovinac and Bilder, 2005).

In stage 9 when the oocyte begins to grow much larger than the nurse cells, the FCE undergoes a dramatic shape change as well. The FCE splits into three populations. Approximately 8 cells at the anterior pole of the chamber, the border cells, separate from the other FCs and begin a migration through the nurse cells towards the oocyte taking along the anterior polar cells as well (Figure 2)(Montell 2003). The remaining FCs split into two populations, one of squamous cells, and one of columnar cells. Most of the FCE takes on a columnar shape, forming tall narrow cells, placing most follicle cells in contact with the growing oocyte. The FCs transform from a nearly uniform distribution around

the nurse cells and oocyte to two distinct populations where approximately 850 FCs will surround the oocyte, and 50 FCs will surround the nurse cells (see Results for further details). This can occur because as the majority of FCs becomes columnar and appear to move over the oocyte, the remaining FCs take on a squamous shape enabling their stretch over the remainder of the egg chamber. By stage 10, this differentiation into squamous and columnar cells is distinct, and clearly divided by the nurse cell and oocyte border. This process of columnarization during stage 9 has been characterized as ‘posterior migration’, and is the focus of our study.

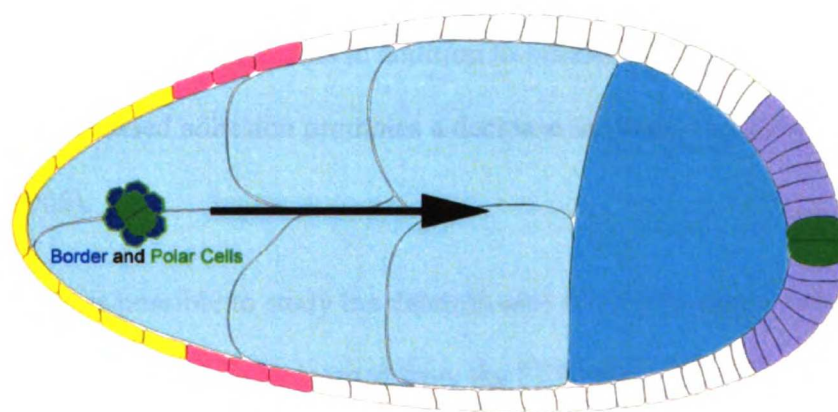


Figure 2. Border cell migration. During stage 9 of oogenesis, the border cells separate from the epithelial layer, and migrate between the nurse cells. The cluster will reach the oocyte at the beginning of stage 10, its location for the remainder of oogenesis (Illustration from (Horne-Badovinac and Bilder, 2005)).

Although in wild type egg chamber behavior it appears that contact with the oocyte causes columnarization, there is evidence to the contrary. In *Bicaudal-D* mutants where the oocyte is small, columnar FCs are located over the nurse cells, and mutations exist that cause squamous cells to be located over the oocyte (Gonzalez-Reyes et al., 1995; Roth et al., 1995; Swan and Suter, 1996). We seek to better understand this process

known as posterior migration, and have used a quantitative and mechanics-based approach to complement the genetic techniques usually applied to study this system.

Understanding this transition from cuboidal to squamous and cuboidal to columnar shape has been difficult because of a lack of mutations that disrupt the process. Some information has been gained from mutant FCs without β h-spectrin. The *Karst* gene encodes β h-spectrin, which is part of the apical membrane skeleton. Additionally, the mutation results in the breakup of the *zonula adherens* (Zarnescu and Thomas, 1999). In *karst* mutants, fewer columnar epithelial cells come in contact with the oocyte than in WT chambers. The previous interpretation of this mutation is that it prevents constriction of the apical side of the follicle cells in addition to interfering with adhesion. The impact of this is that decreased adhesion promotes a decrease in lateral surface area (Foty and Steinberg, 2005).

While it is possible to study the determinants of cellular morphology in typical adult tissues, there is much to be learned from the FCE where the morphology is rapidly changing. As well, the *Drosophila* FCE is genetically accessible to organism wide mutations and genetic mosaic techniques that can produce mutations in small and specific populations of cells within the egg chamber, making the system ideal for study. It is an excellent tool for the study of epithelium in general, as it shares characteristics of both adult and embryonic cells. The FCE is in fact an adult tissue, but its behavior in terms of function and movement are reminiscent of embryonic epithelium and their role in morphogenesis.

3. Overall project goals

The body of *Drosophila* research is immense, and contributions to the techniques available to *Drosophila* researchers can be especially impactful. *Drosophila* research has been especially productive in uncovering the biological mechanisms of development, where the function of a multitude of genes has been characterized. Oogenesis is often studied because of the powerful genetic techniques that can be utilized, and the ease with which data can be collected. Although we have taken a mechanics-based approach to studying the system, we have also drawn from the wealth of genetic techniques by using an enhancer trap fly line in order to identify populations of cells in the FCE. Additionally, our understanding of the system would not be possible without the wealth of research into the genetic and molecular basis of development.

Our goal is to develop new quantitative techniques for the study of biological systems, and to apply them to the study of oogenesis. This work offers insights that are not apparent when studied with genetic manipulation and microscopy alone. We hope the techniques we developed here can be applied to other systems to help in the development of new biological hypotheses, and the testing of other existing hypotheses.

4. The goal of this thesis

This thesis sets out to establish the relevance of studying *Drosophila* oogenesis and the FCE, describe the techniques we have developed to study the system, and explain the conclusions we have made regarding FC behavior. We have chosen to focus upon the process whereby the FCE separates into populations of squamous and columnar cells.

We have studied the FCE using quantitative techniques that have not previously been applied to the system. Specifically, we have quantitatively characterized the morphology of the FCE using confocal microscopy, and incorporated conclusions made from this data in conjunction with previous work into a representative finite element mechanical model of the system.

Past characterizations of stage 9 follicle cell displacement

1. Posterior migration

During stage 9 of oogenesis the initially cuboidal FCE divides into populations of squamous and columnar cells. This has previously been described as ‘posterior migration’ because it appears that the cuboidal cells are migrating toward the posterior pole of the egg chamber and being squeezed into a columnar morphology (Figure 3). This transformation from cuboidal to columnar morphology takes place in a wave beginning at the posterior end of the chamber. Simultaneously, the stretch cells transition from cuboidal to squamous in a wave starting at the anterior pole. Mutations that impact this posterior displacement have been studied; however the results are difficult to interpret. The following sections describe some these mutations, and the conclusions that they imply.

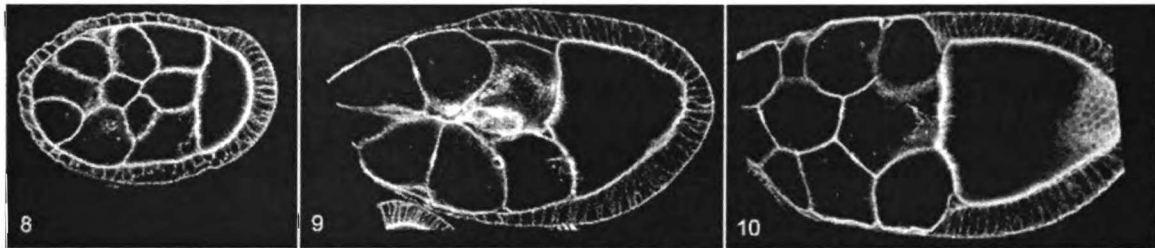


Figure 3. Posterior displacement of follicle cells. At stage 8, the follicle cells are nearly uniformly distributed over the surface of the egg chamber. The morphology of the egg chamber undergoes a transformation during stage 9, and approximately 850 of 900 follicle cells will cover the oocyte by stage 10. The remaining cells that are not situated over the oocyte are of a squamous morphology, and stretch around the nurse cells.

2. Follicle cell displacement depends upon oocyte positioning

This A-P patterning of the FCE seems to be driven by oocyte signaling. The posterior displacement of the FCs results in a layer of columnar cells situated directly

over the oocyte with the border between columnar and squamous cells occurring precisely at the oocyte-nurse cell boundary. The *spindle-C* gene is required for correct positioning of the oocyte, and in mutants the oocyte fails to locate to the posterior 60% of the time (Gonzalez-Reyes and Johnston, 1994) . This can result in the oocyte being located at the anterior of the chamber, or with nurse cells on both sides of the oocyte. In those mutants with centrally located oocytes, the columnar FCs still locate to the surface of the oocyte (Figure 4).

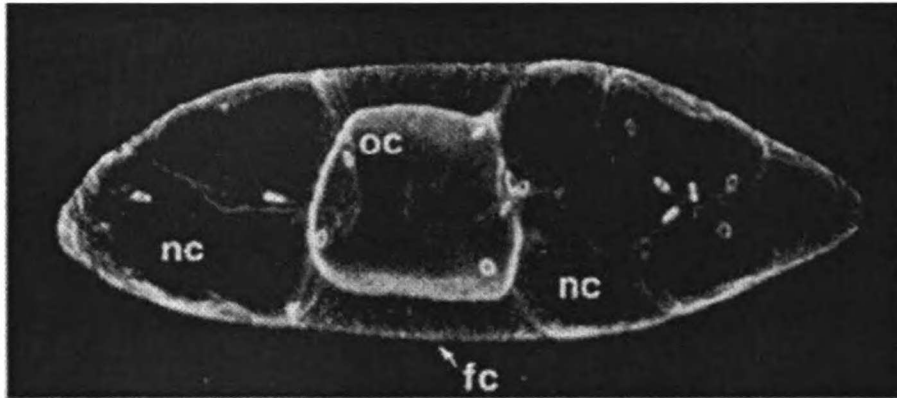


Figure 4. Follicle cell morphology depends upon oocyte positioning. In this spindle-C egg chamber, the oocyte (oc) is abnormally located centrally between the nurse cells (nc). The follicle cells (fc) still displace towards this irregularly located oocyte rather than toward the posterior pole (Gonzalez-Reyes and Johnston, 1994).

3. Apical constriction as a hypothesis for posterior displacement

The dramatic change in morphology seen during the cuboidal-columnar transition has led others to conclude that contraction in the apical domains is necessary for the columnar cells to gather over the oocyte surface. In fact, the area of the apical domains of the columnar fated cells has been described as decreasing during stage 9. This contraction has been attributed to apical constriction, and there is evidence to suggest this to be the case. In *karst* mutants, which lack β_H -spectrin, a component of the membrane skeleton

associated with the apical surface and the *zonula adherens*, cells fail to completely columnarize (Zarnescu and Thomas, 1999). This was attributed to dysfunctional apical constriction and an inability to migrate over the apical surface.

Other work indicates that apical constriction may not be of primary importance to the columnarization. One such manipulation that has been studied is mutation in *spaghetti squash (sqh)*, which encodes the nonmuscle myosin II regulatory light chain (RLC) (Edwards and Kiehart, 1996). This gene is then rescued by a *sqh* transgene rescued by the *hsp70* promoter which is induced by heat shock. These mutants can be rescued to adulthood through daily heat shocking. Long-term depletion of RLC is fatal; however the impact of short-term depletion and myosin's role during various stages can be studied. Both border cell migration and centripetal migration are sensitive to RLC depletion, resulting in border cells that do not reach the oocyte, and centripetal cells that fail to close over the anterior end of the oocyte. In contrast, RLC depletion does not interfere with the cuboidal-columnar transitions. This is initially surprising, and provides some indication that apical constriction may not be necessary for the cuboidal-columnar transition.

Evaluating posterior displacement of the FCE as a migration may be a misclassification. The process appears to lack some of the attributes typical of migration, most notably the polarized extension and contraction of cell bodies. In order to formulate new hypotheses to explain FC behavior, the morphology of these cells must be better characterized and quantified.

Morphometric characterization of the follicle cell epithelium

1. Introduction

The cuboidal-squamous and cuboidal-columnar transitions of stage 9 of oogenesis are complex events. A comprehensive study of the process would necessitate investigation of the morphologies, genetics, signaling, and mechanics that drive the elegant biological process that we observe. With multiple cell types and complexities within each of these aspects, it is necessary to focus on the areas we believe will be most beneficial to understanding the FC behavior. We believe that conclusions regarding what has become known as posterior migration are based upon incomplete morphological data, and that quantification and analysis of cell morphology can lead to valuable insights.

Using confocal imaging it is possible to observe the morphology of follicle cells and egg chambers in great detail. In conjunction with criteria for staging egg chambers, it is possible to infer cell behavior over time as well. By using an enhancer trap fly line and tools we developed for morphometric characterization, we were able to formulate a more complete description of FC morphology during stage 9 than what has previously been done before.

2. Fly Stocks

Drosophila stocks are maintained at room temperature in vials containing moist food. This moist food is a mixture of water, yeast, soy flour, yellow cornmeal, light malt extract, agar, light corn syrup, and propionic acid (Bloomington 2007). The food is designed to sustain the flies during all stages of their development and lasts

approximately 1 month. Dry yeast is added to the surface of the food prior to the addition of flies to the vials.

For our investigation, it is desirable to dissect well-nourished, young female flies, which have a greater number of healthy follicles upon dissection. It is also desirable to control the nutrition level, as this can have a significant impact upon the size and quality of the egg chambers. In order to study only young flies, the following procedure is used.

Vials with large numbers of flies in the pupal stage are selected. The adult flies are then removed from the vials, leaving only those flies in the pupal and earlier stages. The next day, the newly hatched flies are transferred to a vial of fresh food. These flies are then transferred to a vial of fresh food and dry yeast every other day until 7 days after their initial separation, at which time they are dissected. This results in well nourished young flies of nearly the same age.

3. *Drosophila* strains

A fly line was chosen to enable the identification of the boundary between squamous and columnar fated follicle cells. It has previously been established that the *dpp* gene is expressed in the follicle cells with squamous fate starting late during stage 8 of oogenesis (Twombly et al., 1996). Using an enhancer trap line where *lacZ* is inserted into the *dpp* gene, β -galactosidase is produced in those cells expressing *dpp*. β -galactosidase can then be detected with antibody staining enabling the identification of those cells with squamous fate. The complete genotype for this fly strain is *cn[1]P{ry[+t7.2]=PZ}dpp[10638]/CyO; ry[506]*, which is available from the

Bloomington Stock Center (Bloomington 2007). These flies are expected to behave as wild type flies in all ways except *lacZ* expression.

4. Dissection

Flies are anesthetized by filling the food vials with CO₂. The flies are then removed from the vial and placed upon a CO₂ venting pad. Females are then selected for dissection by visual identification. Dissection is done manually with forceps in phosphate buffered saline (PBS) under a dissecting microscope. The ovaries are dissected from the flies under a dissecting microscope due to the small size of the fly and the ovaries.

First, the fly is grasped with forceps between the abdomen and thorax (Figure 5). The end of the abdomen is then pinched with a second pair of forceps, and this end is pulled in the posterior direction. This will ideally pull out the ovaries in addition to a section of the gut. Often the ovaries are not removed, and they must be removed by gently squeezing the abdomen to massage out the ovaries. The gut if present is then separated and the ovaries can be collected for further preparation.

Once the ovaries are removed, they must be combed to partially break the muscle sheath (Figure 6). This serves the purpose of allowing better antibody penetration for the subsequent fluorescent imaging. Also, the egg chambers will ideally be separated from the muscle sheath and the other chambers before they are imaged, and combing at this stage will assist in the future separation of the chambers. When performed properly, combing results in less tightly bunched ovarioles that are still connected to the ovary.

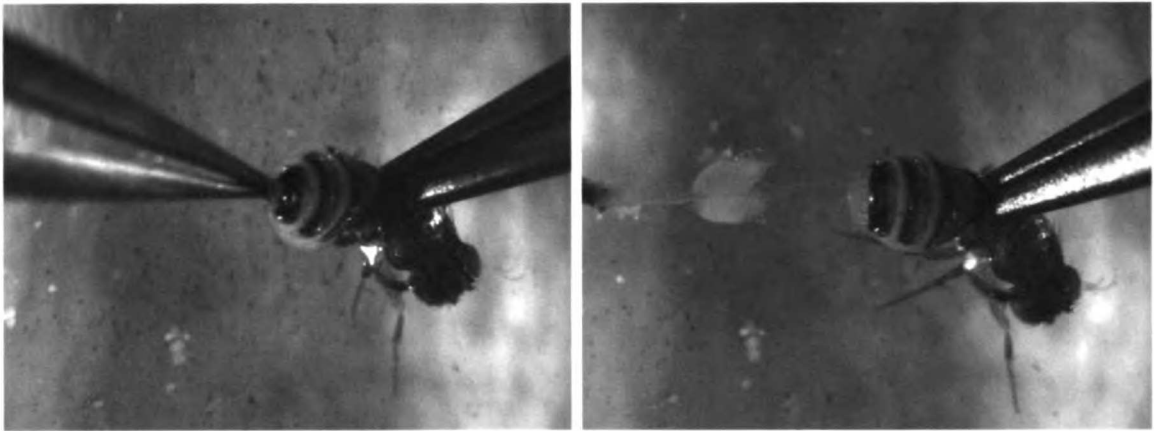


Figure 5. Dissection of Drosophila ovaries. By pulling on the ovaduct, the ovaries are removed in a pair from the posterior of the fly. A section of the gut is typically intertwined with the ovaries and must be separated.

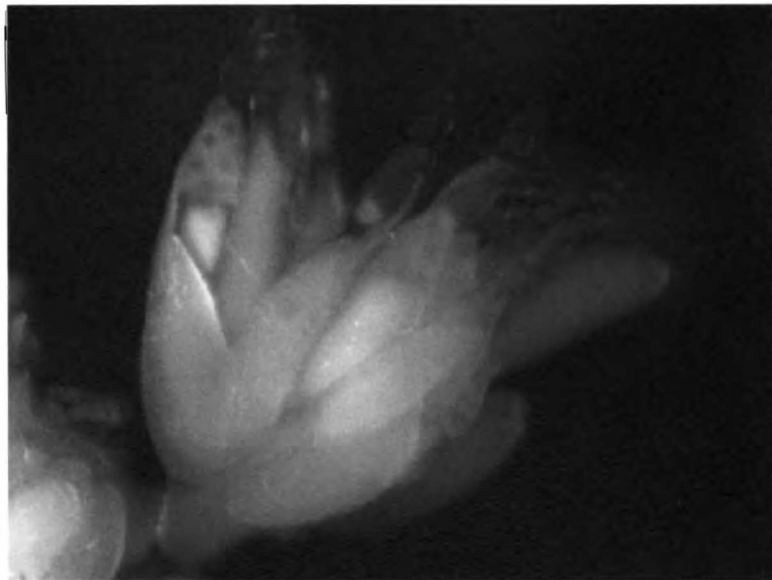


Figure 6. A well combed ovary. This ovary has been combed in order to break up the muscle sheath. The chambers can be seen in all of the successive stages of development in order from the top right to bottom left of the image. Note the growth present between the earliest and latest stages.

5. Fixation and staining

Before the egg chambers can be observed with the confocal microscope, they must be fixed and stained. After being dissected from the flies, the ovaries are fixed in

4% EM grade formaldehyde (Polysciences Inc.) in PBS for 15 minutes on a rocker plate. The ovaries are then washed twice in 0.1% Triton X-100 in PBS.

In order to visualize the *dpp-lacZ* expression and the apical boundaries of the FCs, antibody staining is necessary. The ovaries are first blocked in 5% Normal Goat Serum (Vector Labs) and 0.1% Triton X-100 in PBS for 20 minutes on a rocker plate. The ovaries are then incubated in 5% Normal Goat Serum, 0.1% Triton X-100, and the primary antibodies in PBS. The antibodies used were rabbit anti- β -galactosidase (Biogenesis) at 1:2000 and rat anti-E-cadherin (Developmental Studies Hybridoma Bank). The ovaries are incubated overnight at 4°C on a rocker plate. After incubation, the ovaries are washed 3X in 0.1% Triton X-100 in PBS for 15 minutes. The chambers are then blocked as previously stated, then incubated in 5% Normal Goat Serum, 0.1% Triton X-100, and the secondary antibodies in PBS for 3 hours on a rocker plate. The ovaries are then washed 3X in 0.1% Triton X-100 in PBS for 15 minutes.

After staining, the ovaries must be broken up. The egg chambers are organized in ovarioles within the ovaries, and the individual chambers must be separated for proper visualization. The ovaries and egg chambers are pipetted into a 200 μ L pipette repeatedly until they are separated. The chambers are then placed upon a glass slide by pipette with 15 μ L of Prolong Gold antifade reagent (Molecular Probes). A coverglass is then placed on top of the chambers, and sealed with clear nail polish. A stack of five pennies is placed upon the coverglass to flatten the chambers for improved image quality. By slightly flattening the chambers, a larger number of FC apices could be imaged within the same plane during confocal microscopy.

6. Confocal Imaging

Confocal imaging is a technique which enables microscopy within a narrow imaging plane. Out of plane information is excluded, and optical sections of three-dimensional objects can be acquired. This is of tremendous benefit for egg chamber imaging because cross sections can be visualized easily. As well, it was important to quantify the area of the apical faces of cells, which is aided by imaging the cells in a narrow plane that contains the cell apices.

Egg chamber image acquisition is performed using a Leica TCS laser scanning microscope. Two types of images are acquired: midplane images are captured in order to quantify follicle cell heights. As well, images of the apical domains are acquired through the acquisition of a series of images, because the apices are situated in multiple imaging planes. This is used to quantify cell apical area. Imaging of the apical domain is confirmed by the presence of E-cadherin staining which is present primarily in the adherens junctions of the cells.

7. Morphometric analysis

Morphometric analysis is completed using scripts written in MATLAB 7.4. Using these scripts, *dpp-lacZ* expression boundary, A-P axis length, FC layer height, apical area, and cell volume are all quantified.

A-P axis length, FC layer height, total FC areas, FC volumes, and *dpp-lacZ* expression boundary are calculated from midplane images, while individual cell areas are measured by apical cross sections. Total follicle cell areas are calculated using the area of the follicle cell layer height as rotated about the A-P axis. FC volumes are calculated

similarly, as the difference between the volumes of the basal and apical domains as rotated about the A-P axis. A correction factor is applied to account for squashing of the egg chamber beneath the coverslip.

The boundary of *dpp-lacZ* expression is measured in order to better compare cell morphology data at varying stages. This serves as a marker for cells of squamous fate, which enables us to apply our analysis to only the columnar fated cells where desired. Using this boundary as the origin of our plots, the normalized position of an individual cell should remain relatively constant compared to measuring position with respect to the anterior pole. Details of the morphometric analysis can be found in the Master's thesis of Peter White (White, 2007).

8. Results

Previous work has attributed the cuboidal to columnar transition of stage 9 to migration of the FCs towards the posterior of the chamber, however our data represent a significant departure from previous descriptions of the stage. Our measurements show that for the columnar fated FCs, the total areas of the apical domains significantly increase between late stage 8 and stage 10 (Figure 7).

The area of the columnar fated cells represents a decreasing fraction of the total FC area as the chamber develops. As well, the height to width aspect ratio is increasing. This may have led to the previous erroneous assessment that the columnar cells were decreasing in apical area.

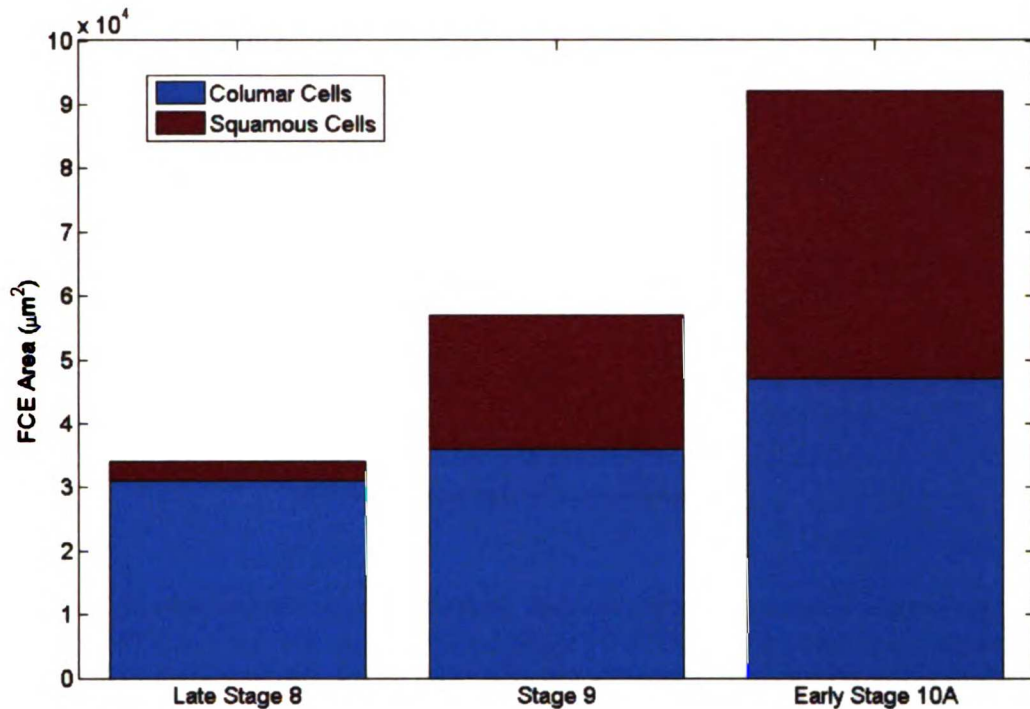


Figure 7. Areas of columnar and squamous follicle cells. The areas of both the squamous and columnar FCs increases over time from stage 8 to stage 10. It was previously reported that the columnar FC area decreases during the posterior displacement of these cells, however our data indicate a contrary conclusion.

Additionally, our data indicate that not only is total columnar FC apical area increasing over time, but there is no indication that any individual cells experience an apical contraction of area either (Figure 8). The cell area curves indicate the greatest areas at the anterior end of the egg chamber, and as expected the steepness of the curve decreases over time. During late stage 8 and stage 9 the cells are in a transitional period, and it appears that the anterior most columnar cells are stretched to their stage 10 areas earlier than the posterior most cells. The dramatic change in cell heights without a corresponding decrease in apical area can be explained by the rapid growth rate that these cells are experiencing (Figures 9, 10).

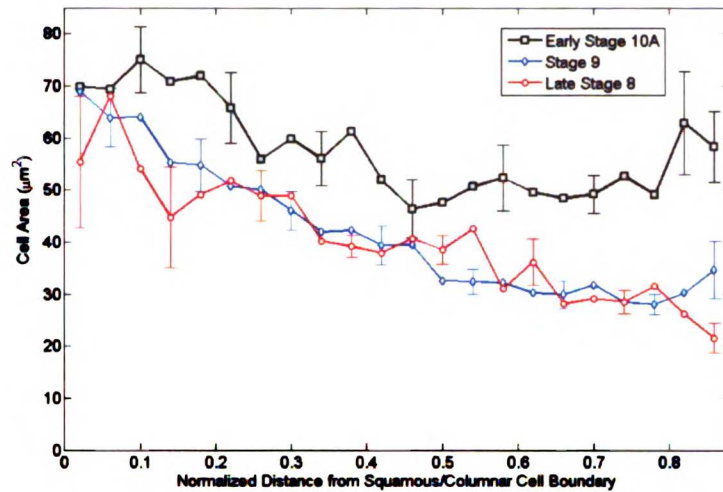


Figure 8. Follicle cell apical areas. The graph indicates that the areas of the apical domains of the FCs are increasing over time. Stage 10 areas are greater than stages 8 and 9 across the entire domain. Error bars indicate standard error of the mean (σ/\sqrt{n}).

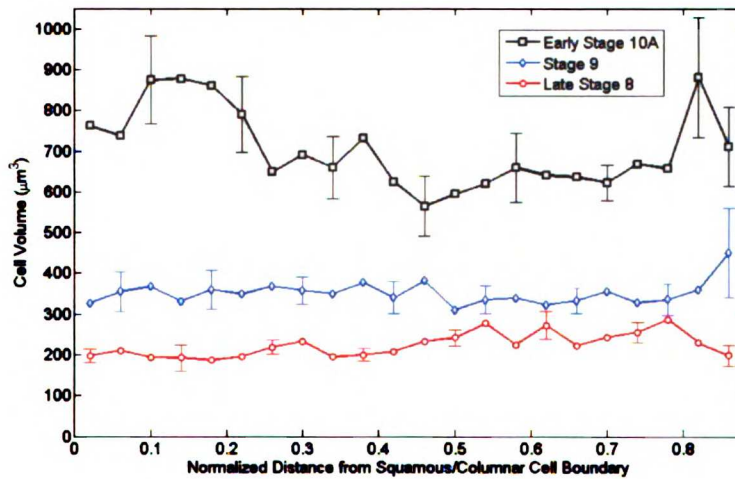


Figure 9. Follicle cell volumes. The follicle cells rapidly increase in volume from stage 8-10. The volume is increasing at a proportionally higher rate than apical areas; therefore the cells must transition to a columnar configuration. Error bars indicate standard error of the mean (σ/\sqrt{n}).

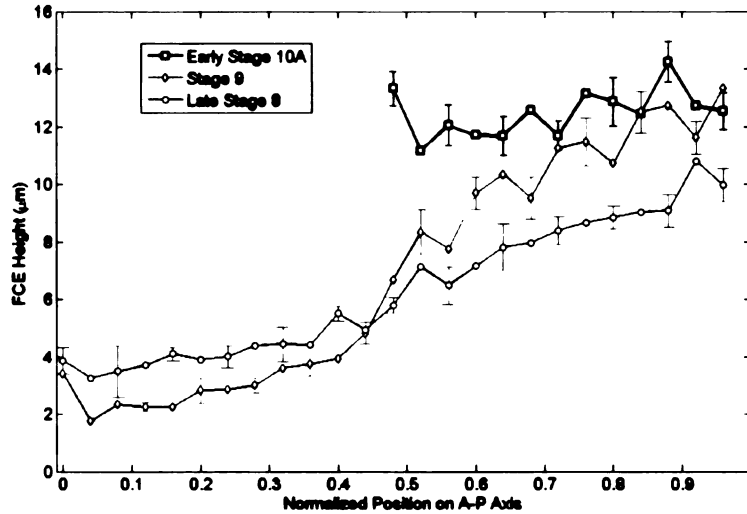


Figure 10. Follicle cell heights. The heights of the columnar fated FCs increase from stage 8-10. Those cells located most posteriorly increase in height soonest. Stage 10 areas are only reported for columnar cells, as the squamous cells required separate imaging techniques and were characterized separately. Error bars indicate standard error of the mean (σ/\sqrt{n}).

9. Conclusions

Our morphometric characterization has led to new perspectives regarding the cuboidal-columnar and cuboidal-squamous transition events observed during stage 9. Our data show that the columnar cells are not decreasing in apical area, suggesting that apical constriction may not be the primary contributing mechanism to the apparent posterior displacement of the columnar follicle cells. As well, this indicates that the columnarization is not responsible for the extension of the stretch cells; instead this can be attributed to growth within the germ-line. The germ-line cells, especially the oocyte, are growing rapidly during this stage, exerting a stretch force upon the FC layer. The FC layer must grow in apical area in order to maintain a continuous epithelium over the surface of the egg chamber (Figure 11).

This behavior can be explained from a molecular perspective as well. It has been previously established that E-cadherin expression strongly increases in columnar fated FCs just prior to their cuboidal-columnar transition. Simultaneously, levels of E-cadherin in stretch cells decrease, and there is remodeling of the adherens junctions (AJs) (Grammont, 2007). The AJ is not only an adhesive structure, but it is also important to the organization of the actin-based cytoskeleton. The reinforcement or diminishment of the AJs forms a molecular and structural basis for varying degrees of extensibility within these cells. Those cells that are reinforced apically resist apical stretch induced by the growing germline and their own growth in volume (see Figure 11).

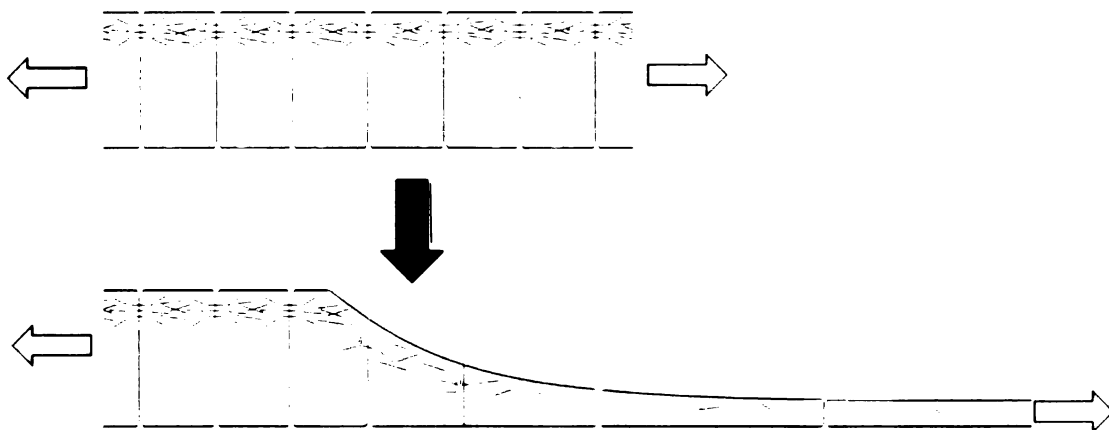


Figure 11. Adherens junctions resist stretch. As the germ-line grows, it exerts a stretch force upon the FC layer. The ability to resist stretching can be attributed to AJ and actin cytoskeleton architecture. Those cells with reinforced AJs restrict the increase in area of their apical domains, while the stretch cells with remodeled AJs are unable to resist their extension.

The ability to resist stretch due to adhesive and cytoskeletal organization is also in line with previous work regarding the dependence upon myosin for the migratory events of oogenesis. While border cell migration and centripetal migration are both highly

sensitive to myosin levels, the columnarization of FCs seems to occur normally under conditions of diminished myosin II levels (Edwards and Kiehart, 1996). If apical constriction were the driving force behind columnarization, a dependence upon myosin for the process would be expected.

Previous work in developmental mechanics modeling

A handful of models have been produced that are capable of representing morphological processes. One group of models is based upon the differential adhesion hypothesis, first formulated by Steinberg in the 1960s. This hypothesis states that cellular segregation is a product of cell surface tensions resulting from differential intercellular adhesion (Steinberg, 1963). There is a subset of experiments and cell behaviors that can be captured by the differential adhesion hypothesis, and it is best suited towards explaining the arrangement and segregation of cells.

The best example of a differential adhesion model system is that of L cells with controlled expression of P-cadherin and N-cadherin. In the experimental system, expression of P-cadherin and N-cadherin was modulated, and the behavior was observed as the cells formed aggregates. As predicted by the differential adhesion hypothesis, those cells with greater cadherin expression and the highest surface tensions formed an aggregate that was surrounded by the cells of lower cadherin expression. As well, computational models based upon differential adhesion capture the experimental results extremely well (Foty and Steinberg, 2005).

Finite element models that implement the essentials of differential adhesion have been used as well (Brodland, 2004). These models implement interfacial tensions between cells in conjunction with effective cytoplasmic viscosity. One positive aspect of these models with respect to epithelial modeling is their ability to exchange membrane between the different surfaces of the cell. This is capable of representing some aspects of

morphogenesis, but it is not sophisticated enough to capture the processes of *Drosophila* oogenesis.

The next class of model used to capture epithelial behavior is continuum-based models. An excellent example of this is Oster's model of sea urchin invagination using the finite element method. Using this technique it was possible to simulate a variety of proposed mechanisms for the invagination. As an output of the model, depending upon the mechanism being simulated, the necessary mechanical properties within the system could be calculated (Davidson et al., 1995). As a follow up to this work, the mechanical properties were measured experimentally (Davidson et al., 1999). The two studies in conjunction made it possible to test the plausibility of different mechanisms for invagination. This implementation is of particular interest because it tests the hypothesis of apical constriction as the driving force for sea urchin invagination, with the prevailing hypothesis for posterior migration being apical constriction as well. This work has served as an inspiration for our own, with the methodology of hypothesis driven finite element modeling with the goal of determining the system's mechanical properties.

This type of model has great potential for oogenesis modeling, but it still lacks some necessary components. One limitation is the use of elastic material properties. Elastic material properties make large morphology changes impossible in the presence of physiologically realistic forces.

There is precedent for use of viscoelasticity in finite element models for the cell (Karcher et al., 2003). Developmental mechanics models need to incorporate aspects from all of the previously mentioned works, as aspects of adhesion, tension generation,

and viscoelasticity are all components of *in vivo* systems. Additionally, growth and time varying mechanical properties are necessary components that have not been applied to developmental computational modeling.

Mechanical description of the FCE and germline cells during oogenesis

1. FCE cytoskeletal and adhesive structures

The mechanics of the FCE can be attributed to a number of cytoskeletal and adhesive structures, but of primary consideration are the AJs and the associated actin cytoskeleton. Located at the boundary between the apical and basolateral domains of epithelial cells, the AJ serves as a junction for cell-cell adhesion in epithelial sheets and is a location for assembly of the actin-based cytoskeleton.

The AJ is composed of three types of proteins: E-cadherins, β -catenin, and α -catenin. Cell-cell adhesion occurs through the extracellular domain of E-cadherin. β -catenin strongly associates with the intracellular domain of E-cadherin, and α -catenin associates with β -catenin. α -catenin has previously been shown to interact with actin, however details of the interaction of actin and the assembled AJ are relatively unknown (Figure 12) (Yamada et al., 2000).

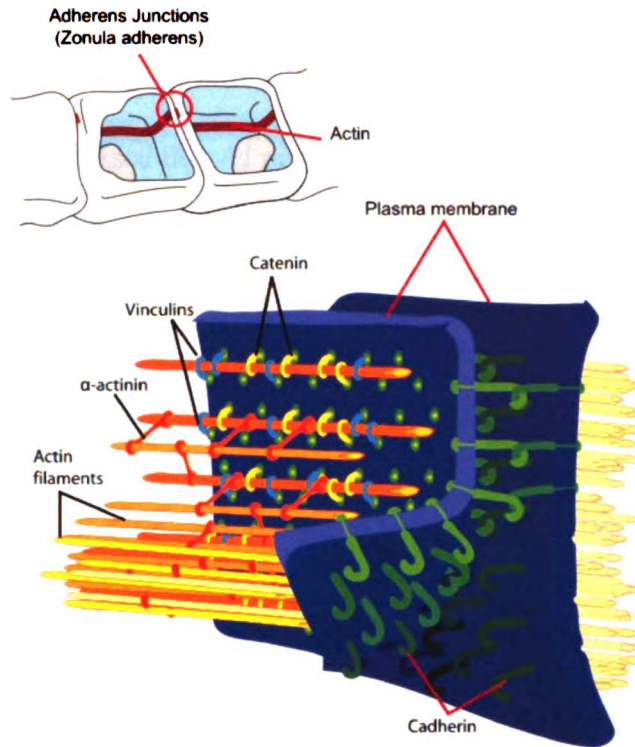


Figure 12. Diagram of adherens junction structure. Located in a band at the boundary of the apical domain, the AJs are comprised of cadherin, α -catenin and β -catenin. α -catenin has been shown to associate with the actin cytoskeleton, and the AJ acts to structurally reinforce the cell (Figure from Ruiz, 2006).

In addition to being a prominent epithelial structure, the AJ has been shown to have a critical role in the shape changes that occur in the FCE from stage 8-10 in the developing egg chamber. Disassembly of the AJs can be found in the stretch cells prior to flattening, while reinforcement of the AJs is found in those cells transitioning to a columnar morphology (Grammont, 2007). Likewise, one mutation has been found that specifically interferes with the cuboidal to columnar transition (Zarnescu and Thomas, 1999). The mutation is for the gene coding β_H -spectrin, a component of the membrane skeleton, which causes subsequent disruption to the AJs. We have interpreted these findings in conjunction with our morphometric data to mean that the adherens junctions

act to resist stretch in the FCE. As such, the AJ is a crucial element in any mechanical description of the FCE.

We have hypothesized that AJ remodeling and reinforcement respectively results in increased and diminished viscoelastic properties. We believe the transition from cuboidal to squamous occurs because of AJ remodeling, and a decreased capacity to resist stretch. Conversely, those cells that will become columnar have enhanced ability to resist stretch as a result of AJ reinforcement.

2. Active force generation and myosin

During stage 9, the FCE splits into three populations. Approximately 8 cells at the anterior pole of the chamber separate from the other FCs and begin a migration through the nurse cells towards the oocyte. The remaining FCs split into two populations, one of squamous cells, and one of columnar cells. During stage 10, a group of the most anterior columnar FCs elongates and migrates towards the center of the chamber in order to separate the oocyte from the nurse cells. These three processes are known as border cell migration, posterior migration, and centripetal migration respectively.

Although all three have been characterized as migration, based upon our data we believe ‘posterior migration’ to be a misnomer. Border cell migration and centripetal migration both exhibit the extension and contraction of cells typical of migration, while ‘posterior migration’ does not. It is true that the columnar FCs exhibit a displacement relative to the oocyte and nurse cells, but our data indicates that this can be attributed to the growth of the oocyte without active cellular migration being necessary.

One of the advantages of *Drosophila* oogenesis as a model system is the variety of genetic manipulations that can be performed. One such manipulation that has been studied is mutation in *spaghetti squash (sqh)*, which encodes the nonmuscle myosin II regulatory light chain (RLC) (Edwards and Kiehart, 1996). This gene is then rescued by a *sqh* transgene rescued by the *hsp70* promoter which is induced by heat shock. These mutants can be rescued to adulthood through daily heat shocking. Long-term depletion of RLC is fatal; however the impact of short-term depletion and myosin's role during the various stages of oogenesis can be studied. Both border cell migration and centripetal migration are sensitive to RLC depletion, resulting in border cells that do not reach the oocyte, and centripetal cells that fail to close over the anterior end of the oocyte. In contrast, RLC depletion does not interfere with the cuboidal-squamous and cuboidal-columnar transitions. This is initially surprising, and provides some indication that apical constriction may not be necessary for the cuboidal-columnar transition.

With these results in mind, we have chosen not to incorporate myosin and active force generation into our model of stage 9 follicle cell behavior. While myosin and apical constriction may contribute to follicle cell behavior during this stage, it appears that it would be secondary in importance to what we believe to be growth-mediated displacement.

3. Apical and basolateral division of cell domains

Apical-basal polarity is central to the behavior of epithelial cells and the FCE. In these cells, the cell membranes can be divided into two functionally distinct domains: the apical and basolateral domains (Muller, 2000). In the developing egg chamber, the apical domain of the FCE is responsible for adhesion to the germline cells and for the secretion

of egg shell proteins that will eventually protect the egg (Godt and Tepass, 1998). The AJ and associated cytoskeletal components are located near the apical domain of the cell as well. The basolateral domain is responsible for adhesion to the basement membrane and septate junction cell-cell adhesion. The functional differences between the apical and basolateral domains suggest that they should be distinct within a mechanical description for the FCE as well.

4. Material properties

While little work has been done to characterize the material properties of the FCE, there has been previous work for other epithelial cell types (Yamada et al., 2000). Cells have been shown to exhibit viscoelastic behavior, although there is significant controversy regarding the specifics of a cell material law. The cell's inhomogeneous nature, varying molecules, and active force generation all make a precise material law difficult to develop.

During oogenesis the FCE experiences irreversible deformations and we have chosen the simplest viscoelastic material law to capture this behavior. We have chosen a two parameter Maxwell model, which in 1-D is essentially described by a spring in series with a dashpot, though it should be noted that during the long time scales of oogenesis the FCE primarily behaves in a viscous fashion.

Another important behavior of the FCE is its growth. The entire egg chamber grows significantly during oogenesis, and this cannot be ignored during the stages we are trying to describe. Mass transport occurs from outside the FCE into the FCE and into the

germ-line cells. In lieu of explicitly describing this mass transport, we have chosen to represent growth by thermal expansion. The temperature in the simulated system is not intended to represent the temperature in the real egg chamber, and only influences growth within the system. It is possible to leave out mass transport effects because of the low velocities and lack of momentum effects within the system.

5. Germline characterization

The germline cells of the developing egg chamber have important interactions with the FCE. There is adhesive interaction between the germline and FCE, and cadherin expression can be found on the apical face of the FCE and the follicle cell facing sides of the germline. From stage 8-10 as the oocyte is growing, the oocyte surface is rapidly displacing with respect to the FCE apices. It is unknown what role adhesion between the germline and the FCE plays in this process.

As mentioned earlier, the germline also has the important behavior of growth. From stage 8-10, the nurse cells and especially the oocyte are experiencing rapid growth which seems to exert an outward pressure upon the FCE. Direct measurements of internal pressure within the developing egg chamber do not exist, and this description is inferred from stretch of the squamous FCE.

The cytoplasmic contents of the nurse cells and oocyte are continuously interconnected by large ring canals, which grow up to 10 μm in diameter by stage 11 (Tilney et al., 1996). We have therefore assumed that the contents of the germline cells are at a uniform internal pressure within our model. We are only studying stages prior to

nurse cell dumping, and it is possible that gradients in pressure may exist during those stages.

6. Anterior-posterior elongation

After stage six of egg chamber development, a pronounced longitudinal elongation can be observed. The chamber is initially round in shape, but transitions into a lozenge or football shape during development (Figure 13). This has been attributed to the circumferential organization of actin filaments, although there may be other contributing factors (Gutzeit, 1990). In order to limit the number of parameters within the model, we have chosen an isotropic viscoelastic material model; therefore it is not possible to incorporate this behavior with our model. An orthotropic viscoelastic material model could be used to capture this behavior, though this is outside of the scope of this thesis.

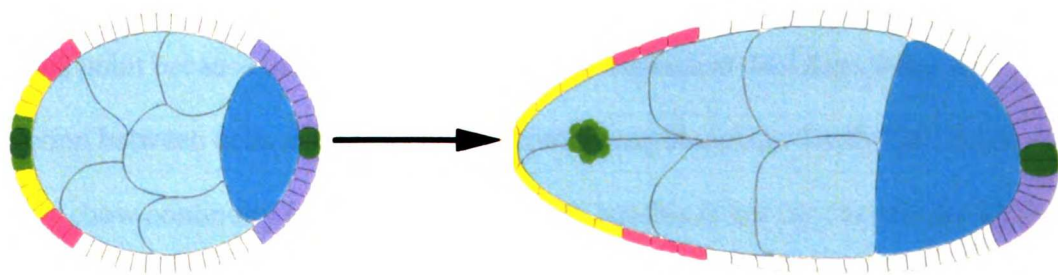


Figure 13. Anterior-posterior elongation. Egg chambers transition from a spherical to elongated shape from stage 6 onwards. The importance of circumferential actin organization has been established; however there may be other contributing mechanisms. It is still unclear what causes the pointed shape at the anterior pole. (Illustration from Horne-Badovinac and Bilder, 2005).

7. Initial and final state of the system

The geometric configurations in our model are based upon the data we have collected through confocal microscopy. As mentioned with respect to A-P elongation, the chamber has an elongated shape. We have not incorporated a material model capable of modeling this aspect of the egg chamber, and our geometric data has consequently been adapted for use within the model. While stage 8 egg chambers are already significantly elongated, we have adapted the shape of the chamber to be spherical in its initial configuration. If we were to implement the elongated shape, the system would return to a spherical shape due to the uniform pressure loading and isotropic material model.

We have chosen to model chambers from early stage 8 to early stage 9 configurations, before the pronounced boundary between columnar and squamous cells is observed. As stage 9 progresses, the anterior FCs make a transition from flattened cells to squamous cells in a wave proceeding from the anterior end forward. As this takes place, apical continuity is lost between adjacent cells (Figure 14). The FCE was simulated only up to this point because there is currently a lack of biological data describing the connection between cells at this apically discontinuous boundary. Epithelial sheets typically show continuity in their apical domains, but this is not the case for the FCE (Baker and Garrod, 1993). The significance of this behavior is not apparent, and there is a tremendous opportunity to study the adhesive structures present after adherens junction breakdown at the boundary between columnar and squamous cells.

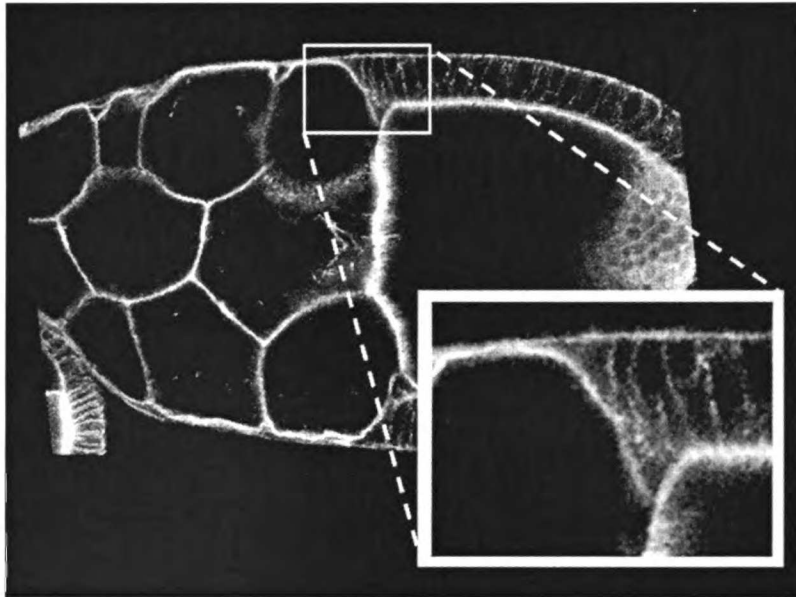


Figure 14. Apical discontinuity in a stage 10 egg chamber. At the boundary between squamous and columnar cells, continuity between apical domains is lost. The architecture of the remaining junction is currently unknown.

Concurrent with the gap in biological data, the discontinuity in cell boundaries cannot be well incorporated into our continuum model for the FCE. In order to include this behavior within a finite element model, criteria for the separation of boundaries must be established, in addition to a characterization of the connection that remains between the cells.

Finite element model implementation

1. Preprocessor and solver

All models were generated in ADINA v8.3.1 (Automatic Dynamic Incremental Nonlinear Analysis, ADINA R&D Inc., Watertown, MA). ADINA is a software package for performing displacement and stress analyses using the finite element method. The software includes implementations for a variety of material models and is capable of modeling thermal effects as well. This includes the temperature dependant viscoelastic material formulations, which we have used to simulate the FCE. A Lagrangian formulation for large stress and large strain was utilized.

2. Material model

As stated above, we have chosen a continuum formulation for a two parameter Maxwell material model. Additionally, we have utilized thermal strain effects to model growth within the system, and temperature dependent viscoelastic properties using the Williams-Landel-Ferry shift function (Bathe and ADINA R & D, 2005).

The viscoelastic formulation is due to Holzapfel, which is a generalized Maxwell model with many chains (Figure 15)(Holzapfel, 1996). These chains are comprised of springs with stiffness E and dashpots of viscosity η . In our implementation, E^∞ is chosen to be negligibly small, and only one chain represented by E^1 and η^1 in the figure is utilized. Previously established material constants were used for the baseline apical domain properties, with $E = 300\text{Pa}$ and $\eta = 100\text{Pa}\cdot\text{s}$ (Karcher et al., 2003). The model was constructed with elevated properties in the apical domains, with $\eta = 2000\text{Pa}\cdot\text{s}$, with the material properties degrading to their baseline levels sequentially over time starting at

the anterior pole. The most anterior region of the model has baseline material properties throughout the entire simulation. The timing of the transition for the remainder of the follicle layer from elevated to baseline material properties was iterated until the simulated output matched our morphometric data.

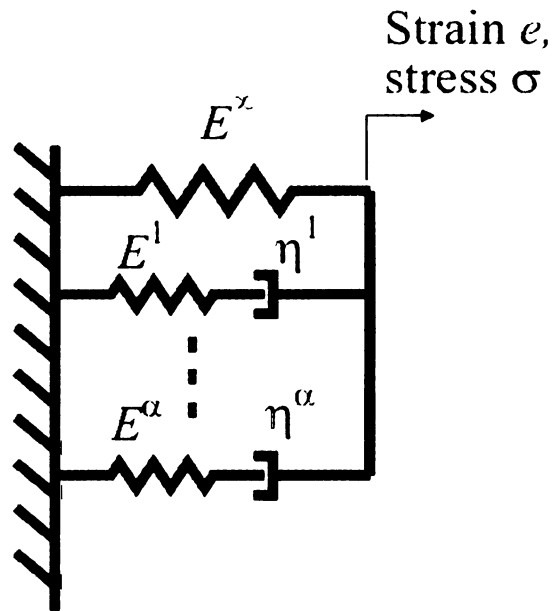


Figure 15. Generalized Maxwell material model. The Holzapfel formulation is for a generalized Maxwell material of many chains. In our model, a two parameter model with only one chain was utilized (Bathe and ADINA R & D, 2005).

Material properties of different magnitudes could be chosen, which would lead to a change in the required internal pressure and the timing of the material property transition. While the model would behave differently, this would not lead to changes in the conclusions of the model. Our model serves as a demonstration of our hypothesis for FC behavior, and the material properties are not expected to be predictive of those found in the *in vivo* follicle cells.

While the FCE does not experience significant temperature effects *in vivo*, thermal effects were used for the purpose of the finite element implementation. Thermal strain effects were used to model growth within the system. The thermal strain, e_{th} , is calculated using the following equation:

$$e_{th} = \alpha(\theta)(\theta - \theta_{ref}) \quad (\text{Eq. 1})$$

where α is a material constant, and θ is temperature. The temperature induced strain is assumed to be isotropic. For our simulations, $\alpha = 0.2$ and $(\theta - \theta_{ref})$ varies linearly from 0 to 1.65 over the simulation time. This captures the volumetric growth observed from stage 8 to 9. This must be applied only to the basolateral domains of the simulated cells as the apical domains are growing in area at a rate slower than the volumetric increase, hence the columnarization.

Generating the model, it was determined that this isotropic growth contributes to stretch in the apical domains. With basolateral domain material properties of the same magnitude as apical properties, it was impossible to sufficiently restrict stretch in the columnar cells while simultaneously generating the appropriate deformation in the stretch cells. Consequently, the basolateral domain was modeled with severely deficient properties in order to capture the growth behavior without impacting the level of apical domain stretching. The properties used for the domain are $E = 0.3\text{Pa}$ and $\eta = 0.1\text{Pa}\cdot\text{s}$.

In order to simulate time varying material properties, another thermal effect was utilized. A Williams-Landel-Ferry shift function (Bathe and ADINA R & D, 2005) was applied to the apical domains in order for the viscosity of the domain to be controlled by

temperature. This is governed by the following equations, where C_1 and C_2 are material constants, and T_0 is a reference temperature:

$$a_T = \frac{\eta(T)}{\eta_0(T_0)} \quad (\text{Eq. 2})$$

$$\log a_T = \frac{-C_1(T - T_0)}{(T - T_0 + C_2)} \quad (\text{Eq. 3})$$

In our model, $C_1=2.602$, $C_2=10$, and $T_0=0$. To diminish the viscosity, the temperature of the domain shifts from 0 to 10 resulting in a 20-fold decrease in domain viscosity from $\eta = 2000\text{Pa}\cdot\text{s}$ to $\eta = 100\text{Pa}\cdot\text{s}$.

3. Forces exerted by the germ-line

The effect of the germ-line on the FCs is modeled as internal pressure. This pressure is exerted uniformly at a magnitude of 4.0×10^{-4} Pa, which was calculated in order for the anterior-most cell to stretch. Though this is a very low pressure, it is sufficient as the deformations occur over the period of 6.25 hours.

4. Meshing and solution

The model is meshed with 1288 9-node 2-D axisymmetric elements. This implementation assumes the egg chamber is axisymmetric along the A-P axis, an assumption that remains reasonable until stage 10 of oogenesis. The mesh is separated into 23 domains, approximately the number follicle cells spanning from pole to pole along one arc. This enables the variation of material properties within domains similar to the size of a cell. The apical domain has an initial thickness of $1\mu\text{m}$, and the basolateral

domain had a thickness of $7\mu\text{m}$. The initial A-P axis length is $107\mu\text{m}$. The dynamic model spanned 6.25 hours of simulated time.

5. Results and discussion

The model simulates the growth and stretch experienced by the FCE. Using a minimal description that includes viscoelastic material properties that diminish over time, uniform growth, and a stretch inducing internal pressure, it is possible to recreate the bulk of the FCE morphological behavior. The initial and deformed meshes show the pronounced stretch that occurs at the anterior pole of the follicle, and the increase in height at the posterior pole (Figure 16). The anterior pole is stretched from an initial height of $8\mu\text{m}$ to a final height of $2\mu\text{m}$. The posterior pole increases in height from $8\mu\text{m}$ to $14\mu\text{m}$. Overall chamber length is $159\mu\text{m}$, comparable to the average value of $150\mu\text{m}$ from our confocal imaging data.

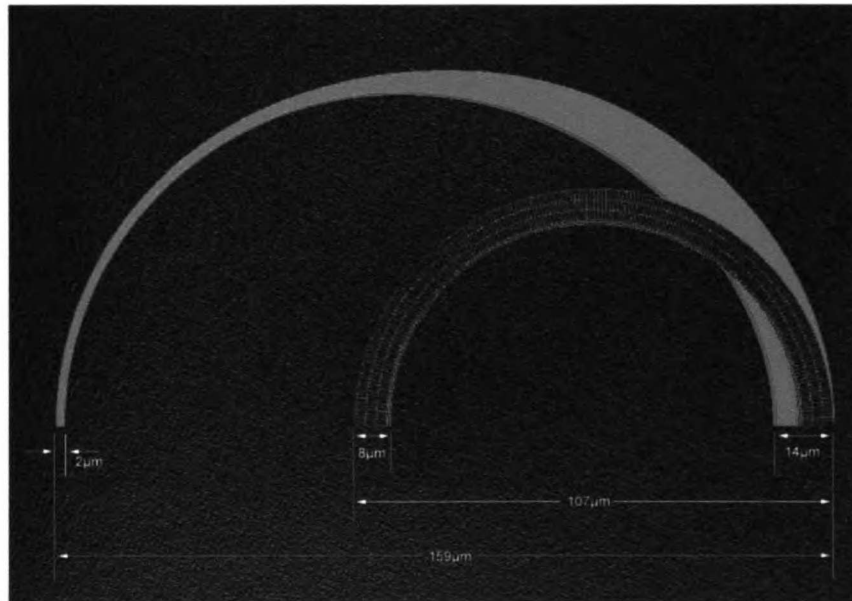


Figure 16. Initial and deformed meshes. Cell morphologies are observed in a gradient of morphologies from squamous to columnar, as observed in the Drosophila egg chamber.

The timing of the viscosity shift is reminiscent of the remodeling of AJs that is observed in the egg chamber, starting from the anterior pole and proceeding in a wave in the posterior direction (Figure 17). The timing of this shift appears to have two separate phases, which may represent independence of squamous and columnar cell behavior. While there is a breakdown of viscosity across the entire chamber, this may not occur *in vivo*, and may represent a mismatch of material properties and internal pressure. For most of the model representative of columnar fated cells, the viscosity diminishes near the end of the simulation, causing the least impact on their total level of stretch.

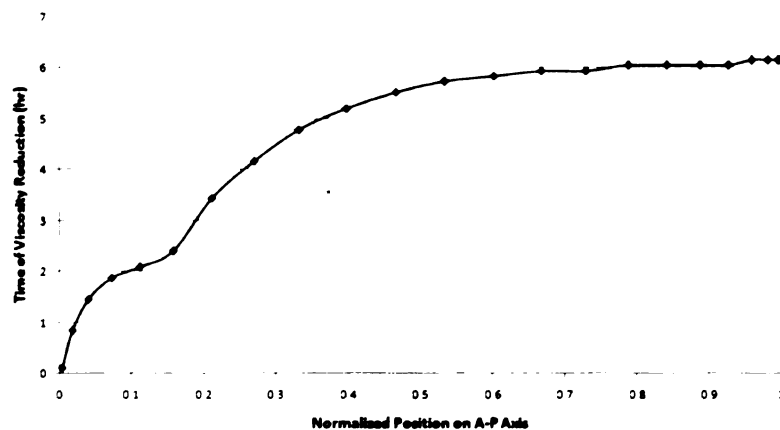


Figure 17. Time of viscosity shift. The viscosity of the apical domains shifts from enhanced properties ($2000\text{Pa}\cdot\text{s}$) to baseline values ($100\text{Pa}\cdot\text{s}$). This occurs sequentially, beginning at the anterior pole. The timing is irregular, and may be representative of two independent behaviors for the squamous and columnar FCs.

The timing of the viscosity shift is optimized in order to match our FC layer height data acquired from confocal imaging (Figure 18). We believe that the real height profile is a smooth function, and that the oscillatory nature of our data is an artifact of the error in our measurements. Consequently, we did not attempt to match the model to our

confocal data precisely over the domain, instead aiming to match the overall trend of the data.

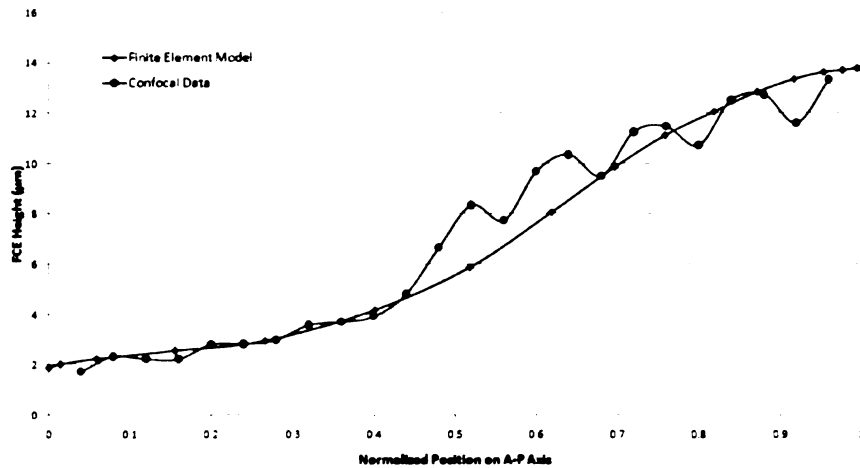


Figure 18. Follicle cell heights. The simulated system matches the trend in heights from morphometric data acquired by confocal microscopy.

One notable difference between the simulated and *in vivo* chambers is the lack of elongation found in the simulated system (Figure 19). Not only is the *in vivo* system elongated, but there is also an additional pointed feature at the anterior pole. Egg chambers have circumferential organization of their actin cytoskeleton, a property which was not represented in our model, therefore elongation was not expected. The mechanism that induces the pointed anterior pole observed in egg chambers is currently unknown as well; therefore there was no attempt to implement this behavior in the model. In future iterations of FC modeling, orthotropic material properties could likely capture the behavior induced by the polarized actin filaments, resulting in a more representative model.

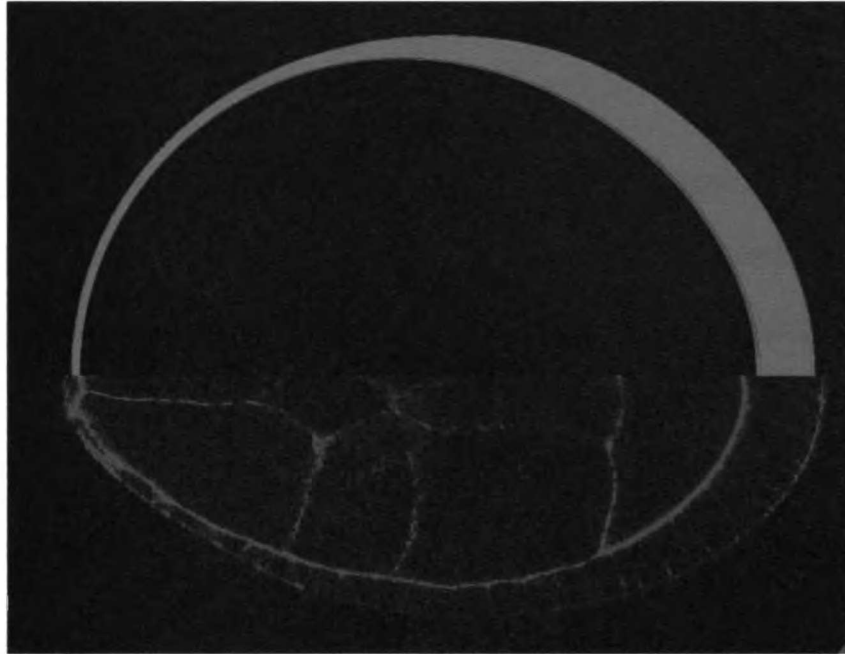


Figure 19. Comparison of simulated and real egg chambers. The simulated system did not capture the elongation present in vivo.

An additional inaccuracy of the model is the deficient material properties assigned to the basolateral domains. When simulated with realistic properties for the basolateral domain, it was not possible to sufficiently resist stretch in the columnar cells. This is likely a result of our implementation for growth within the model, which is for isotropic thermally induced strain. This may be indicative of targeted growth within the follicle cells to induce an increase in height, which would diminish the amount of reinforcement necessary to resist apical stretch.

6. Conclusions and future work

While the behavior of the FCE is complex in nature, the bulk of the morphological behavior can be modeled with a small set of forces and mechanical properties. Although the columnarization of the FCE has been attributed to apical

constriction, our model is the implementation of an alternative hypothesis without any dependence upon apical constriction.

With our morphometric data and analysis, we have shown that the columnar FCE is growing in apical area, and the so-called posterior migration is actually just the oocyte growing and making contact with a greater number of FCs. With this knowledge in hand, it is possible to develop simplified hypotheses that better fit previous experimental works. Significantly, a proposed model for FC columnarization should not have a dependence upon active force generation as the behavior has been shown to occur normally in chambers with depleted myosin II (Edwards and Kiehart, 1996).

Our computational model for FCs is capable of simulating the growth and the changes in height and area observed during stages 8 and 9 of oogenesis. While the model has deficiencies, it is a useful first step toward more comprehensive descriptions, and is useful for testing the plausibility of hypotheses for FC behavior.

Future FC models would be enhanced by more sophisticated implementations of growth and material models. Both of these areas could be enhanced with more realistic computational implementations as well as a greater understanding of the biological detail underlying these properties. Though our material model for the basolateral domain was not a realistic implementation, it indicates the need for a more sophisticated model for growth, and may have biological significance as well. The columnar fated FCs are growing at a rapid rate, yet the rate of apical area growth is severely restricted. This appears to be indicative of targeted growth rather than the isotropic growth model we

have implemented in the model. This may be a possible avenue for future research into mutations that affect targeted growth within epithelia, and their impact upon the FCE.

As well, future implementations could be greatly enhanced by orthotropic material properties. The current hypothesis for the elongation of egg chambers is that the circumferential organization of actin filaments forms a 'molecular corset'. Orthotropic material models specifically for the purpose of describing fibrous materials exist, and could likely capture much of the behavior that is observed. This is limited though, and would likely not explain the pointed shape of the anterior pole. Direct measurement of FC material properties would also be extremely useful to a future description of the system.

References

- Bloomington Drosophila Stock Center. [online] URL: flystocks.bio.indiana.edu
- Baker, J., and D. Garrod. 1993. Epithelial cells retain junctions during mitosis. *Journal of Cell Science* 104:415-425.
- Bathe, K.J., and ADINA R & D. 2005. ADINA Theory and Modeling Guide.
- Brodland, G.W. 2004. Computational modeling of cell sorting, tissue engulfment, and related phenomena: A review. *Appl Mech Rev* 57(1):47-76.
- Chan, H.C. 2001. Epithelial Cell Biology: An Interface with Multidisciplines in Life Sciences. *Cell Biology International* 25(10):991-992.
- Davidson, L.A., M.A.R. Koehl, R. Keller, and G.F. Oster. 1995. How do sea urchins invaginate? Using biomechanics to distinguish between mechanisms of primary invagination. *Developmental Dynamics* 121:2005-2018.
- Davidson, L.A., G.F. Oster, R.E. Keller, and M.A.R. Koehl. 1999. Measurements of Mechanical Properties of the Blastula Wall Reveal Which Hypothesized Mechanisms of Primary Invagination Are Physically Plausible in the Sea Urchin *Strongylocentrotus purpuratus*. *Developmental Biology* 209:221-238.
- Drummond-Barbos, D., and A.C. Spradling. 2001. Stem Cells and Their Progeny Respond to Nutritional Changes during Drosophila Oogenesis. *Developmental Biology* 231(1):265-278.

- Edwards, K.A., and D.P. Kiehart. 1996. *Drosophila* nonmuscle myosin II has multiple essential roles in imaginal disc and egg chamber morphogenesis. *Development* 122:1499-1511.
- Foty, R.A., and M.S. Steinberg. 2005. The differential adhesion hypothesis: a direct evaluation. *Developmental Biology* 278:255-263.
- Godt, D., and U. Tepass. 1998. *Drosophila* oocyte localization is mediated by differential cadherin-based adhesion. *Nature* 395:387-391.
- Gonzalez-Reyes, A., H. Elliot, and D.S. Johnston. 1995. Polarization of both major body axes in *Drosophila* by gurken-torpedo signalling. *Nature* 375:654-658.
- Gonzalez-Reyes, A., and D.S. Johnston. 1994. Role of Oocyte Position in Establishment of Anterior-Posterior Polarity in *Drosophila*. *Science* 266:639-642.
- Grammont, M. 2007. Adherens junction remodeling by the Notch pathway in *Drosophila melanogaster* oogenesis. *The Journal of Cell Biology* 177(1):139-150.
- Gutzeit, H.O. 1990. The Microfilament Pattern in the Somatic Follicle Cells of Mid-Vitellogenic Ovarian Follicles of *Drosophila*. *European Journal of Cell Biology* 53:349-356.
- Holzapfel, G.A. 1996. On Large Strain Viscoelasticity: Continuum Formulation and Finite Element Applications to Elastomeric Structures. *International Journal for Numerical Methods in Engineering* 39(22):3903-3926.
- Horne-Badovinac, S., and D. Bilder. 2005. Mass Transit: Epithelial Morphogenesis in the *Drosophila* Egg Chamber. *Developmental Dynamics* 232:559-574.

- Karcher, H., J. Lammerding, H. Huang, R.T. Lee, R.D. Kamm, and M.R. Kaazempur-Mofrad. 2003. A Three-Dimensional Viscoelastic Model for Cell Deformation with Experimental Verification. *Biophysical Journal* 85:3336-3349.
- Lauffenburger, D.A., and A.F. Horwitz. 1996. Cell Migration: A Physically Integrated Molecular Process. *Cell* 84:359-369.
- Margolis, J., and A. Spradling. 1995. Identification and behavior of epithelial stem cells in the *Drosophila* ovary. *Development* 121:3797-3807.
- Muller, H.-A.J. 2000. Genetic Control of Epithelial Cell Polarity: Lessons From *Drosophila*. *Developmental Dynamics* 218:52-67.
- Roth, S., F.S. Neuman-Silberberg, G. Barcelo, and T. Schupbach. 1995. *cornichon* and the EGF receptor signaling process are necessary for both anterior-posterior and dorsal-ventral pattern formation in *Drosophila*. *Cell* 81(6):967-978.
- Ruiz, M. 2006. Adherens Junction Structural Proteins. [online] URL:
http://en.wikipedia.org/wiki/Image:Adherens_Junctions_structural_proteins.svg
- Steinberg, M.S. 1963. Reconstruction of tissues by dissociated cells. *Science* 141:401-408.
- Swan, A., and B. Suter. 1996. Role of Bicaudal-D in patterning the *Drosophila* egg chamber in mid-oogenesis. *Development* 122:3577-3586.
- Tilney, L.G., M.S. Tilney, and G.M. Guild. 1996. Formation of Actin Filament Bundles in the Ring Canals of Developing *Drosophila* Follicles. *The Journal of Cell Biology* 133(1):61-74.

Twombly, V., R.K. Blackman, H. Jin, J.M. Graff, R.W. Padgett, and W.M. Gelbart.

1996. TGF- β signaling pathway is essential for *Drosophila* oogenesis.

Development 122:1555-1565.

White, P. 2007. Mechanics of Epithelial Morphogenesis in *Drosophila melanogaster*

Oogenesis: New Insights Based on Quantitative Morphometric Analysis and

Mechanical Modeling. *M.S. Thesis, The University of California, Berkeley.*

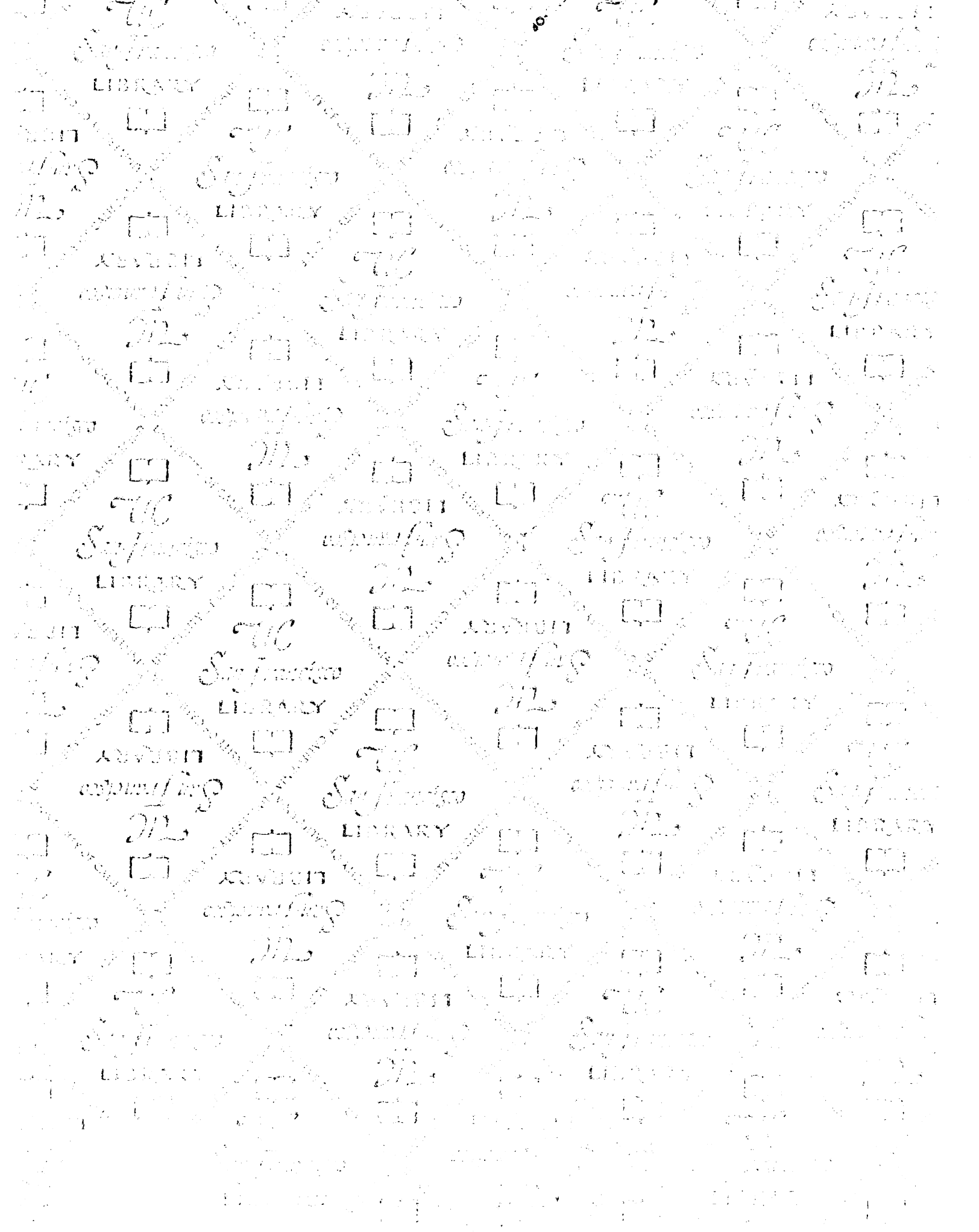
Yamada, S., D. Wirtz, and S.C. Kuo. 2000. Mechanics of Living Cells Measured by

Laser Tracking Microrheology. *Biophysical Journal* 78:1736-1747.

Zarnescu, D.C., and G.H. Thomas. 1999. Apical Spectrin Is Essential for Epithelial

Morphogenesis but Not Apicobasal Polarity in *Drosophila*. *The Journal of Cell*

Biology 146(5):1075-1086.



7075818



3 1378 00707 5818

LIBRARY
USE ONLY

